

Activity report based on CPU time and storage used on PDC and NSC of 2023/2024

Axel Brandenburg (Nordita)

October 11, 2024

In this activity report, we describe and list some highlights of the 26 papers that all acknowledge NAISS. Out of those, 3 are submitted. For the calculations, we use the PENCIL CODE, which is hosted on github <https://github.com/pencil-code>. The Pencil Code Collaboration consists of currently 38 developers who have published their effort in JOSS, the Journal of Open Source Software **6**, 2807 (2021).

Here and below, the 3-digit numbering of the papers coincides with that of Brandenburg's full list of publications on <http://www.nordita.org/~brandenb/pub>. Those preceded by the letter B are also in that list, but under invited conference proceedings. All the papers quoted below acknowledge SNIC, PDC, and/or NSC.

1 Shocks and turbulence in collisionless astrophysical plasmas

Under a strong radiation field (such as close to black holes) the turbulence dynamics is altered due to strong radiative cooling. In order to understand the non-linear behavior of turbulent plasma in such a strong radiation environment, we have performed pioneering radiative kinetic turbulence simulations [1]. This in turn, will help us understand, for example, particle acceleration and heating of diluted plasmas near black holes and neutron stars.

In realistic astrophysical environments, one can expect the upstream plasma not to be homogeneous as assumed in these studies but, to present perturbations or even to be turbulent. How upstream turbulence affects the shock properties and particle acceleration is to date an open question. Using the Runko code, we have studied how a relativistic magnetized shock responds to upstream density perturbations and found, unlike previous works, evidence of particle acceleration [2].

We have also investigated the conversion from electric to magnetic energies, which is relevant to the epoch of reheating in the early Universe [446].

The following papers presenting our results have appeared:

- [1] Pjanka, P., Demidem, C., Veledina, A.: 2023, "Shock Corrugation to the Rescue of the Internal Shock Model in Microquasars: The Single-scale Magnetohydrodynamic View," *Astrophys. J.* **947**, 57
- [2] Demidem, C., Nättilä, J., & Veledina, A.: 2023, "Relativistic Collisionless Shocks in Inhomogeneous Magnetized Plasmas," *Astrophys. J. Lett.* **947**, L10
- 446. Brandenburg, A., & Protiti, N. N.: 2023, "Electromagnetic conversion into kinetic and thermal energies," *Entropy* **25**, 1270

2 Gravitational waves and early universe magnetic fields

An important activity involves the computation of the stochastic gravitational wave background from the Big Bang. Those can be measured in future with LISA and the pulsar timing array. We have continued studying the chiral magnetic effect and have now calculated the resulting GW production [453]. The accuracy of the so-called sound-shell model of gravitational wave production is examined in [453], where we also find a new source of departures. In [442], we computed the effects of departures from general relativity on the spectrum of turbulence-sourced gravitational waves.

- 453. Brandenburg, A., Clarke, E., Kahniashvili, T., Long, A. J., & Sun, G.: 2024, “Relic gravitational waves from the chiral plasma instability in the standard cosmological model,” *Phys. Rev. D* **109**, 043534
- 451. Sharma, R., Dahl, J., Brandenburg, A., & Hindmarsh, M.: 2023, “Shallow relic gravitational wave spectrum with acoustic peak,” *J. Cosmol. Astropart. Phys.* **12**, 042
- 442. He, Y., Roper Pol, A., & Brandenburg, A.: 2023, “Modified propagation of gravitational waves from the early radiation era,” *J. Cosmol. Astropart. Phys.* **06**, 025

3 Turbulent decay and Hosking integral

A major development of the last two years concerns the Hosking integral. It is the correlation integral of the magnetic helicity density. It is conserved and gauge-invariant. Dimensional arguments allow us to determine the power laws of the decays with and without magnetic helicity, and simulations yield the numerical prefactors that are arguably universal [457].

In MHD, the dimensions of the Hosking integral are $\text{cm}^9 \text{s}^{-4}$, but for the Hall cascade, the dimensions are $\text{cm}^{13} \text{s}^{-4}$, which has consequences on the decay [439]. This can have observational implications on the spin-down of pulsars and can explain the temporal increase of the implied magnetic fields from observations [444]. We have now also studied the reality of inverse cascading in simulations of Hall turbulence in spherical shells representing neutron star crusts [459]; see Figure 1.

An important application of decaying turbulence is to the evolution of primordial magnetic fields during the radiation era of the early universe. The turbulent decay stops near the time of recombination after the gas motions have been damped away and the magnetic becomes frozen into the plasma. Remarkably, once we know on which track the field evolves, the endpoints in the diagnostic diagram describe a universal line versus length scale [455]. This line of endpoints depends on some open questions concerning turbulent reconnection (Figure 2) and the physics of radiative damping.

Yet another remarkable situation occurs in chiral MHD [440,448]. To understand the resulting decay, it is important to remember that the real space realizability condition of magnetic

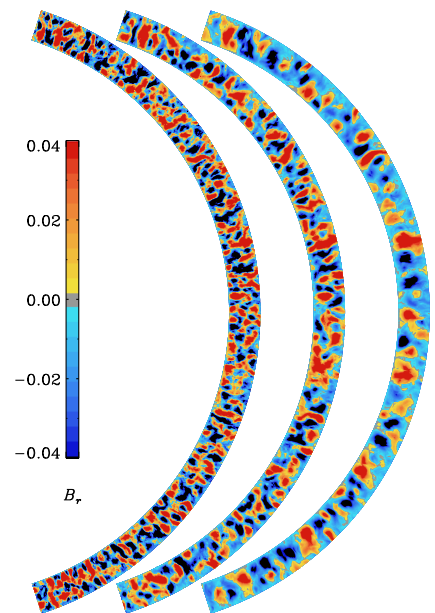


Figure 1: Meridional slices of the radial magnetic field, $B^r(r, \theta)$ at normalized times $\tilde{t} = 6 \times 10^{-7}$, 2×10^{-6} , and 6×10^{-6} (from left to right) in a model of decaying Hall turbulence.

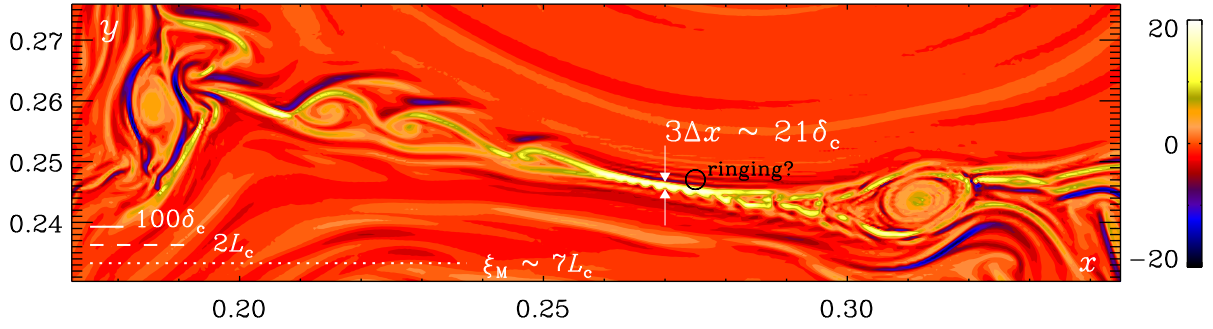


Figure 2: Visualization of perpendicular current density for a run with magnetic Prandtl number $\text{Pr}_M = 10$ and Lundquist number $\text{Lu} = 1.8 \times 10^5$ at 16384^2 mesh points for a small part of the domain with sizes $2.8\xi_M(t) \times 0.74\xi_M(t)$. The lengths of $100\delta_c$, $2L_c$, and ξ_M are indicated by horizontal white solid, dashed, and dotted lines, respectively. The thickness of the current sheet corresponds to about $3\Delta x \approx 21\delta_c$. In its proximity, there are also indications of ringing, indicated by the black circle.

helicity \mathcal{H}_M is always valid and implies $|\mathcal{H}_M| \leq 2\mathcal{E}_M\xi_M$, where \mathcal{E}_M is the magnetic energy density and ξ_M the correlation length. Assuming the inequality to be saturated, we find the scaling $|\mathcal{H}_M| \propto |\langle\mu_5\rangle| \propto t^{-r}$ with $r = p - q = 2/3$, where μ_5 is the chiral chemical potential. The quantity $2\mathcal{E}_M\xi_M/\mathcal{H}_M \approx 1$ is found to be fairly constant, therefore confirming the validity of our underlying assumption. On top of this evolution of the chiral asymmetry, the growth rate of the chiral plasma instability, $\gamma_5 \propto \langle\mu_5\rangle^2 \propto t^{-4/3}$, decays more rapidly than t^{-1} , which causes it to grow less efficiently so as not to spoil the scaling properties of the system.

The conservation of the Hosking integral is not restricted to an initial k^4 spectrum [441], but can also occur for shallower spectra [450]. Furthermore, a non-vanishing mean fermion chirality along with dynamo action can be obtained just from inhomogeneous chemical potential fluctuations [452].

- 459. Dehman, C., & Brandenburg, A.: 2024, “Reality of Inverse Cascading in Neutron Star Crusts,” *Astron. Astrophys.*, submitted (arXiv:2408.08819)
- 457. Brandenburg, A., & Banerjee, A.: 2024, “Turbulent magnetic decay controlled by two conserved quantities,” *J. Plasma Phys.*, submitted (arXiv:2406.11798)
- 455. Brandenburg, A., Neronov, A., & Vazza, F.: 2024, “Resistively controlled primordial magnetic turbulence decay,” *Astron. Astrophys.* **687**, A186
- 452. Schober, J., Rogachevskii, I., & Brandenburg, A.: 2024, “Chiral anomaly and dynamos from inhomogeneous chemical potential fluctuations,” *Phys. Rev. Lett.* **132**, 065101
- 450. Brandenburg, A., Sharma, R., & Vachaspati, T.: 2023, “Inverse cascading for initial MHD turbulence spectra between Saffman and Batchelor,” *J. Plasma Phys.* **89**, 905890606
- 448. Brandenburg, A., Kamada, K., Mukaida, K., Schmitz, K., & Schober, J.: 2023, “Chiral magnetohydrodynamics with zero total chirality,” *Phys. Rev. D* **108**, 063529
- 444. Sarin, N., Brandenburg, A., & Haskell, B.: 2023, “Confronting the neutron star population with inverse cascades,” *Astrophys. J. Lett.* **952**, L21

- 441. Brandenburg, A., & Larsson, G.: 2023, “Turbulence with magnetic helicity that is absent on average,” *Atmosphere* **14**, 932
- 440. Brandenburg, A., Kamada, K., & Schober, J.: 2023, “Decay law of magnetic turbulence with helicity balanced by chiral fermions,” *Phys. Rev. Res.* **5**, L022028
- 439. Brandenburg, A.: 2023, “Hosking integral in nonhelical Hall cascade,” *J. Plasma Phys.* **89**, 175890101

4 Dynamo action in the Sun and Galaxies

To connect our early Universe simulations discussed above with the later cosmological evolution, we have now performed simulations of large-scale structure formation with realistic magnetic fields [438]. In [445], we studied α -type dynamo in non-equilibrium turbulence. A major reviews of galactic dynamos has appeared in [443], and one on the Sun in [447].

- 447. Brandenburg, A., Elstner, D., Masada, Y., & Pipin, V.: 2023, “Turbulent processes and mean-field dynamo,” *Spa. Sci. Rev.* **219**, 55
- 445. Mizerski, K. A., Yokoi, N., & Brandenburg, A.: 2023, “Cross-helicity effect on α -type dynamo in non-equilibrium turbulence,” *J. Plasma Phys.* **89**, 905890412
- 443. Brandenburg, A., & Ntormousi, E.: 2023, “Galactic Dynamos,” *Annu. Rev. Astron. Astrophys.* **61**, 561–606
- 438. Mtchedlidze, S., Domínguez-Fernández, P., Du, X., Schmidt, W., Brandenburg, A., Niemeyer, J., & Kahniashvili, T.: 2023, “Inflationary and phase-transitional primordial magnetic fields in galaxy clusters,” *Astrophys. J.* **944**, 100

5 Axionlike particle–photon conversion in MHD simulations

The conversion of axionlike particles (ALPs) and photons in magnetized astrophysical environments such as galaxy clusters provides a promising route to search for ALPs. We have presented the first systematic study of ALP–photon conversion in more realistic, turbulent fields from dedicated magnetohydrodynamic (MHD) simulations [449], which we compare with Gaussian random field (GRF) models. We find that the MHD models agree with the exponential law for typical, small-amplitude mixings but exhibit distinctly heavy tails for rare and large mixings. We explain how non-Gaussian, local spikes in the MHD magnetic field are mainly responsible for the heavy tail. The results indicate that limits placed on ALPs using GRFs are conservative but that MHD models are necessary to reach the full potential of these searches.

- 449. Carezza, P., Sharma, R., Marsh, M. C. D., Brandenburg, A., Müller, E.: 2023, “Magnetohydrodynamics predicts heavy-tailed distributions of axion-photon conversion,” *Phys. Rev. D* **108**, 103029

6 Small-scale dynamo turbulence

We have continued to study small scale dynamos both in forced and decaying non-helical turbulence and have shown that the Hosking integral, describing the correlation of magnetic helicity

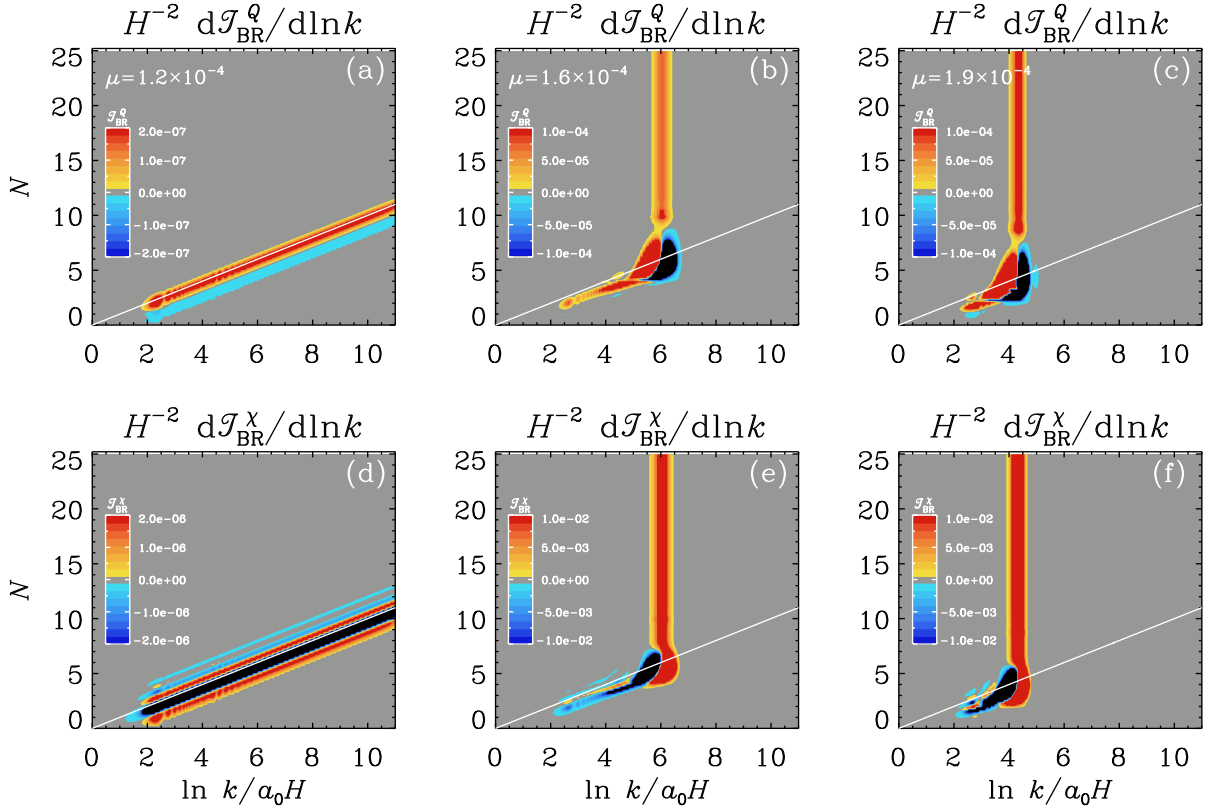


Figure 3: The integrands of the backreaction integrals, denoted here by $d\mathcal{T}_{\text{BR}}^Q/d\ln k$ and $d\mathcal{T}_{\text{BR}}^X/d\ln k$, respectively, as a function of wavenumber k (normalized by a_0H , where a is the scale factor and H the Hubble parameter) and the number of e -folds N for models with gauge field mass parameter $m_Q = 2.44$, panels (a) and (d), where backreaction is negligible, $m_Q = 3.58$, panels (b) and (e), and $m_Q = 4.19$, panels (c) and (f). The white line indicates the position of the comoving horizon. The plots show the development of superhorizon models above the white line when backreaction is important.

fluctuations, this gauge-invariant and conserved in non-helical turbulence. In driven turbulence, the small-scale dynamo develops a $k^{3/2}$ Kazantsev spectrum, which is well known. We have now shown that in the kinematic regime of the dynamo, it connects to a very steep k^4 Batchelor spectrum, which turns to a shallower k^2 Saffman spectrum as the dynamo saturates. The turning point is the integral of scale of turbulence. We have studied its diagnostics properties in terms of the rotational invariant E and B polarizations [435]. To our surprise, the two are very different from each other, especially at large magnetic Prandtl numbers Pr_M . In [436], we also show that the ratio of wavenumber of dissipative to viscous structures is $k_\eta/k_\nu = (\text{Pr}_M/\text{Pr}_M^{\text{crit}})^{1/2}$, where $\text{Pr}_M^{\text{crit}} \approx 0.27$.

436. Brandenburg, A., Rogachevskii, I., & Schober, J.: 2023, ‘‘Dissipative magnetic structures and scales in small-scale dynamos,’’ *Mon. Not. Roy. Astron. Soc.* **518**, 6367–6375
435. Brandenburg, A., Zhou, H., & Sharma, R.: 2023, ‘‘Batchelor, Saffman, and Kazantsev spectra in galactic small-scale dynamos,’’ *Mon. Not. Roy. Astron. Soc.* **518**, 3312–3325

7 Backreaction of axion-SU(2) dynamics during inflation

We have recently explored the effects of backreaction on a model of axion-SU(2) inflation, where we found the emergence of a novel attractor, supported by the backreaction of super-horizon gauge field modes on the rolling axion [454]. This novel backreaction-supported attractor was found numerically; see Figure 3. The strength and correlation length of the resulting helical magnetic fields depend on the inflationary Hubble scale. For suitable parameter choices we find that the strength of the resulting magnetic fields having correlation lengths around 1 Mpc, consistent with the required intergalactic magnetic fields for explaining the spectra of high energy γ rays from distant blazars [460].

- 460. Brandenburg, A., Iarygina, O., Sfakianakis, E. I., & Sharma, R.: 2024, “Magnetogenesis from axion-SU(2) inflation,” *J. Cosmol. Astropart. Phys.*, submitted (arXiv:2408.17413)
- 454. Iarygina, O., Sfakianakis, E. I., Sharma, R. & Brandenburg, A.: 2024, “Backreaction of axion-SU(2) dynamics during inflation,” *J. Cosmol. Astropart. Phys.* **04**, 018

8 Astrobiology and chemical reactions

With the PENCIL CODE, we can perform simulations of chemical reactions. The spreading of COVID-19 is in principle one such example. This led us to understand why the spreading of COVID-19 follows a piecewise quadratic growth.

- 437. Brandenburg, A.: 2023, “Quadratic growth during the COVID-19 pandemic: merging hotspots and reinfections,” *J. Phys. A: Math. Theor.* **56**, 044002

The spatial spreading of COVID, which was already discussed in previous PDC and NSC reports, is also covered there and in a new paper [437], where we investigate the effects of reinfections on the spreading in a spatially extended two-dimensional model.

Academic achievements

PhD student Yutong He has successfully defended his PhD thesis on 4 June 2024. On 16 June 2023, Gustav Larsson defended his Bachelor’s thesis, and Nousaba N. Protiti defended her Master’s thesis on 13 October 2023.